Fractals from Hinged Hexagon and Triangle Tilings

H. A. Verrill

Warwick University, UK; H.A.Verrill@warwick.ac.uk

Abstract

The starting point in this article is a variant of the Smith Truchet tiling, with tiles hexagons or triangles, with an arc design on each tile. A hinged procedure is applied. When repeated indefinitely, families of fractals are obtained. These are terdragon fractals, their boundary, and Sierpinski triangle variations. The Koch snowflake also appears. This is a continuation of the construction of fractal dragons from hinged Truchet tilings in a Bridges 2023 paper.

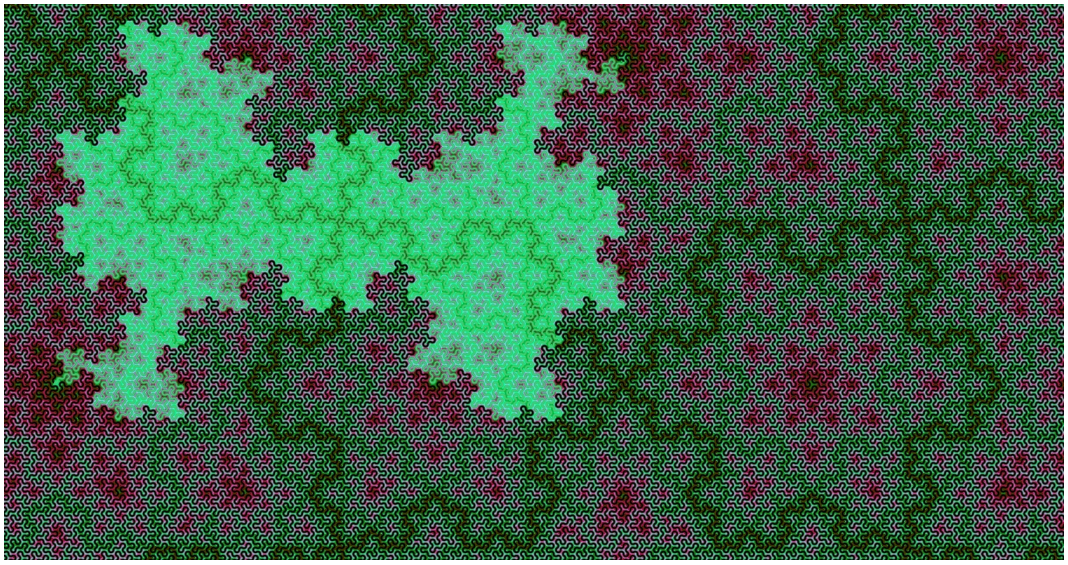

Figure 1: *Terdragon fractal curves and Koch snowflakes obtained from a hinged hexagon tiling.*

Hinged Tilings

In [9], a hinged procedure was applied to Smith Truchet square tilings to obtain fractal dragons. Many other hinged tilings exist [4] [5], [7]. The hinged square tiling is simplest, since after opening to the maximal amount, we obtain another square tiling. A tiling of hexagons does not immediately hinge. However, with

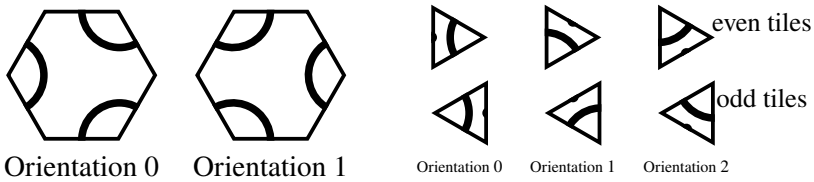

Figure 2: *Hexagon and triangle variants of the Smith Truchet tile.*

the addition of links, we can obtain a hinged hexagon tiling, shown in Figure 4, up to scaling. At the maximal extent of opening, Figure 4 (f), we obtain a new hexagonal tiling. A tiling of equilateral triangles does hinge. The gaps between the tiles, when the tiling is opened sufficiently, can be dissected into equilateral triangles,

as in Figure 13. Thus, starting with either hexagon or triangle tilings, with Smith Truchet like tile designs, as in Figure 2, we are able to proceed iteratively, and produce fractal structures.

Most of the images in this paper and the supplement [10] were produced by the programs at [11]. Clicking on "preset" buttons in that program will recreate these images. The parameters can be varied to change the images in a continuous manner. The art work should be considered dynamic rather than static, therefore fixed images in this paper can not completely convey the result, but give a feeling for the continuous (in the sense of varying the iteration level continuously) and variable (in the sense of changing colours, styles, path) nature of the results. Therefore, although this paper gives many different images, they should all be considered to be parts of the same multidimensional piece of art.

Fractals from Hinged Hexagon Tilings

We start with a hexagonal Truchet tiling, as in Figure 3 (a). The 30° clockwise hinged operation is shown in

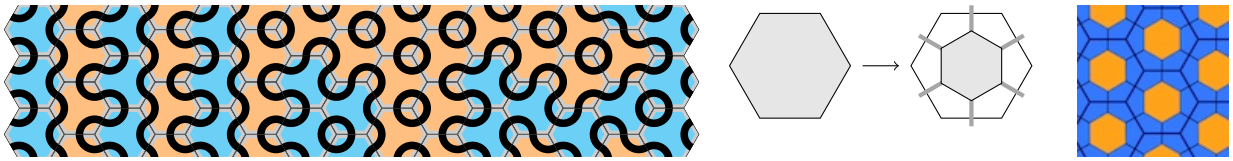

Figure 3: *(a) Hexagon Smith Truchet tiles. Orientation determines tile colour. (b) Tile replacement rule. (c) Result of replacement rule applied to Figure 4 (a).*

Figure 4, (a) to (f). In a physical hinged tiling, the tiles all remain the same size. However, we scale down the tiles, by a factor of $\sqrt{3}$ from one generation to the next. There is also a comparable counterclockwise operation. We call these operations 1 and 0 respectively. In Figure 4 (a) we have an initial tiling of orange

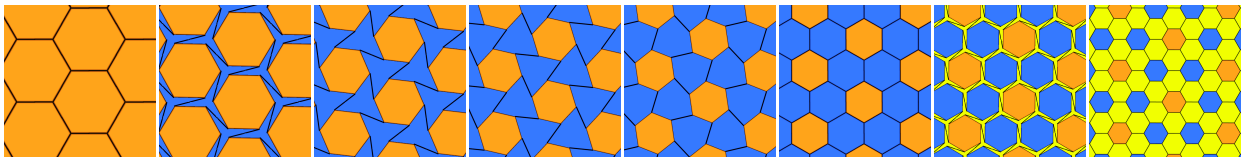

Figure 4: *Hinged hexagons with links, clockwise rotation, operation* 1. *The stage of operation is given by the value of t. Completed operations are obtained with whole number values of t.*

hexagons on a blue background. The background becomes visible once the linked tiles start to rotate. At the maximally open position of the hinging operation, Figure 4 (f), the background becomes newly created foreground tiles. Now the operation can be applied again, with a new yellow background colour. In Figure 4, operation 1 is applied twice, once from (a) to (f), and the second time from (f) to (h). The hinging operation gives a continuous way to see the development of a process which could alternatively be achieved by discrete steps, as in Figure 3 (b), and [10, Figure 8]. The images are determined by a choice of a sequence of operations, and stage of operation. For example, 0110 applied to stage 3.5 means apply operation 0, then 1, then 1, then "half" of operation 0, illustrated in [10, Figure 2]. The discrete operation applied to Figure 4 (a) results in Figure 3 (c), which once the outlines of the initial hexagons is removed, gives us Figure 4 (f).

Now we consider tiles with the Truchet design, as in Figure 2, left. Once the tiling is maximally opened, there is a unique path preserving way (depending on which operation is applied) to orient the Truchet

pattern on the newly created tiles. This is shown in Figure 5, where orange indicates orientation 0, and blue

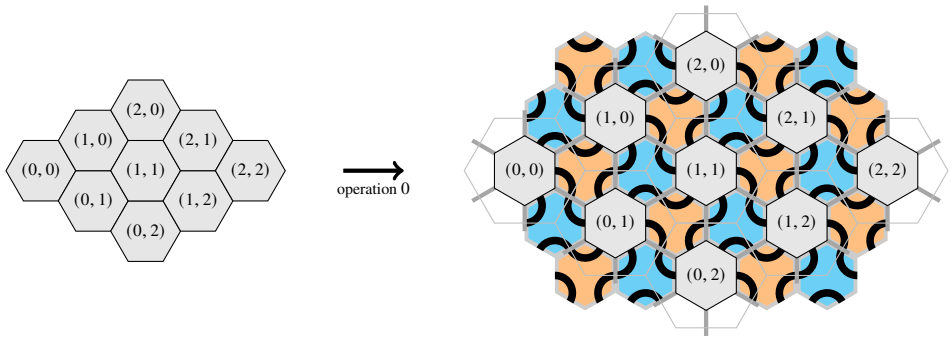

Figure 5: *Diagram showing the tiles added after applying the hinging operation* 0*.*

orientation 1. In order to clearly show how the original tiles end up in the resulting tiling after application of operation 0, Figure 5 right is scaled back up by $\sqrt{3}$, so that the original tiles are the same size as on the left. Connected paths transform to connected paths, via a continuous deformation. An example of application of operations 1 then 0 is shown in Figure 6. A continuation of this figure is shown in [10, Figure 14]. We can

(a) $t = 0$ **(b)** $t = 0.4$ **(c)** $t = 1$ **(d)** $t = 1.6$ **(e)** $t = 2$

Figure 6: *Operation* 1 *followed by operation* 0*, with intermediate steps shown.*

apply the operations 0 or 1 arbitrarily often. For every finite binary sequence we obtain a path from each initial arc. These paths can be modified, by straightening and thickening the arc components, to form tiles, as in Figure 8. For every infinite binary sequence, application of the corresponding operations to each arc of the initial Truchet design results in a space filling curve, with fractal boundary. Each binary sequence gives a different result. Similarly to the families discussed in [6], we have an infinite family of fractal curves. Some examples are shown in Figure 7. These figures tile the plane. They must be translated and rotated through a multiple of 120°, for example, as in Figure 9. Further examples are given in [10, Figure 16]. These tiles are an example of "fractiles", tiles with fractal boundary which tile the plane. See [1] for many other examples of fractiles. In Figure 7, single fractiles are shown for clarity. In Figure 8, an example of a tiling obtained after

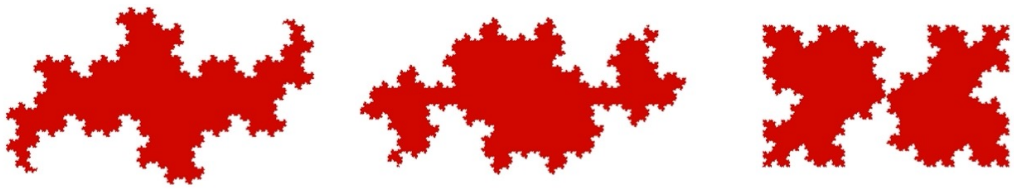

0000000 . . . 001001001 . . . 01010101 . . .

Figure 7: *Fractiles, variants on the terdragon curve, corresponding to binary sequences shown.*

successive application of the operations 1, 0, 1, 0 is shown. In Figure 8, paths composed of thickened straight

lines are used instead of curves, so the circles of Figure 6 (a) become hexagons in Figure 8 (a), covering the background. In Figure 9 each colour tile corresponds to a single initial "arc". See also [10, Figures 18 and

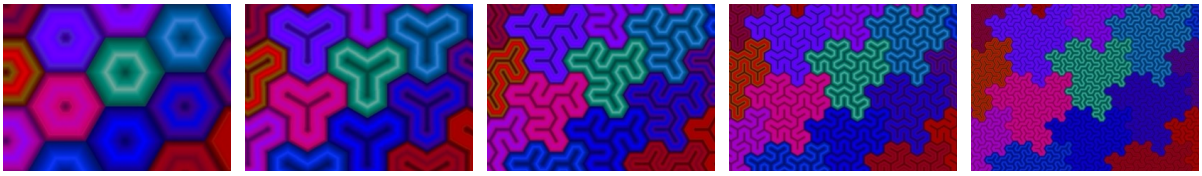

(a) $t = 0$ **(b)** $t = 1$ **(c)** $t = 2$ **(d)** $t = 3$ **(e)** $t = 4$

Figure 8: *Tilings obtained starting from a straight line variant of the Truchet design.*

19]. Figure 9 shows 0, 3 and 6 applications of operation 0 to two different starting arrangements. The first gives a connected but not closed path. The second forms a closed loop. The black outlined hexagon grid is not shown in all images, to avoid clutter. In the limit, it doesn't matter what the exact tile design is; only the

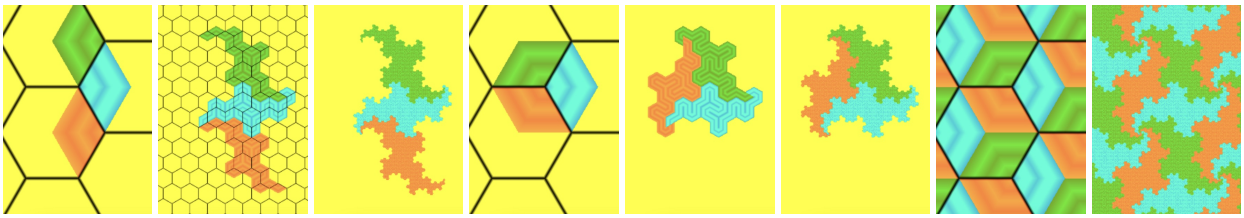

(a) $t = 0$ **(b)** $t = 3$ **(c)** $t = 6$ **(d)** $t = 0$ **(e)** $t = 3$ **(f)** $t = 6$ **(g)** $t = 0$ **(h)** $t = 6$

Figure 9: *Operation* 000000 *applied to different starting configurations.*

dominant colour will show, so either straight lines or arcs end up giving the same results as in Figure 9 (h). These can be recognized as unions of Davis and Knuth's terdragon curve [3, pp. 197, 274], [13]. Originally, the terdragon curve was given by starting from a single line, and iterating of the replacement rule shown in Figure 10 left. This very angular version is replaced by our curved paths. To transform the curved paths to the angular curves, we can use a path consisting of straight line segments from the entry points to the tile centre, shown in [10, Figure 15 (c)]. After sufficiently many iterations, we can't see the difference between curved or straight line segment versions.

Each arc of the initial tiling will converge to a terdragon curve, and so given a hexagon tiling where each tile has three arcs of different colours, we obtain a tiling of the plane given by terdragon curves, as in the approximation in Figure 9 (h). To prove that these are indeed terdragon curves, we look at them in terms of an L-system. An L-system is a sequence of symbols, which may be interpreted as instructions for drawing a path, together with a replacement rule, which means we can iterate from one path to another, more detailed path. Many fractals can be constructed as L-systems [15], [1].

We can give the Truchet paths on the hexagons a consistent direction, as in Figure 10. In contrast to the the square Truchet tiling, where the directions alternate with the parity of the tiles, for the hexagon tiles, all tiles have the same in and out edges. The L-system consists of sequences of the form $X - X - X - \ldots$, where X is either L or R, corresponding "turn left" or "turn right", through 120 degrees. The intermediate dashes, $-$, can be thought of as a path crossing from one tile to the next. To obtain the original terdragon, composed of straight line segments, $-$ would represent a straight line from the centre of one tile to the next. The replacement rule for operation 0 is to replace all occurrences of $-$ by $-R - L-$. For operation 1, we replace $-$ by $-L - R-$. An example of the word corresponding to a particular path is indicated in Figure 10. On entering an orientation 0 tile (orange), you always turn left; on entering an orientation 1 tile (blue), you always turn right. In Figure 5, we see that each path linking from one old tile to the other (the gray tiles)

passes through two tiles of alternate orientation. This corresponds to following direction R then L. For operation 1, we follow direction L then R between the original tiles, shown in [10, Figure 7]. Since it is

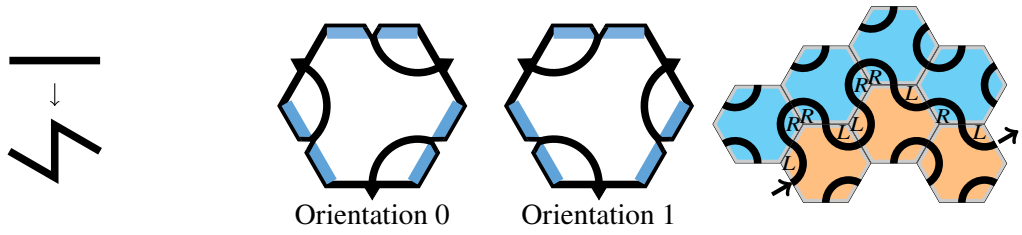

Figure 10: *Left: Original Terdragon replacement rule. Centre: Directions of paths on tiles. Right: A path corresponding to sequence* $L - R - R - L - L - R - R - L - R - L$.

known that the L-system for the terdragon curve has this form [3, 13], we confirm that the space filling curves we have obtained are indeed terdragon curves. The result of repeated application of the operation 0 gives the standard terdragon curve; other binary sequences of operations give other fractals, which we consider to be variants in the terdragon family.

The Koch Snowflake

To obtain the Koch snowflake, we use the tiles with no curves. At each stage, the colour of a point on the image is determined as follows. Let N be the number of hinging operations to be applied. Let $(x, y)_i$ be the coordinate of a point relative to the centre of the hexagon within which it lies at stage i. The colour index of a point is denoted c, and the initial colour of all points is $c = 0$. We start at stage $i = 0$, with an initial tiling where all points are coloured with $c = 0$. In Figure 11 (f), the colours 0, 1, 2, 3, 4 are red, orange, green, dark blue, light blue. In general we need a rule to assign a colour to each positive integer c. The formula used for these images is given in [10, §1.3]. At each stage, the image is divided into a hexagon grid. Each hexagon contains a smaller central, scaled and rotated hexagon. Call this hexagon H. At each stage, a new grid of hexagons is constructed by joining the vertices of the hexagons defined by central hexagons H relative to the previous hexagon grid. In Figure 11, the algorithm to determine colour is shown on the left. Figure 11 (a)

```
1: i ← 0
2: c ← 0
3: while i < N do
4:     if (x, y)_i ∉ H then
5:         c ← c + 1
6:     end if
7:     i ← i + 1
8: end while
```

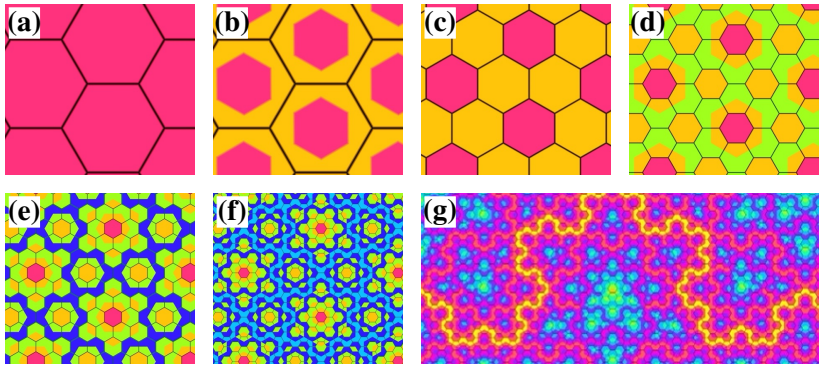

Figure 11: *Iteration algorithm to produce a Koch snowflake tiling, in words and pictures.*

shows the initial tiling. The result of rotating and shrinking the hexagon is shown in (b). For points in the central hexagons, $(x, y)_i \notin H$, the colour is unchanged. For other points, the colour index is advanced by 1, in this case to orange. Next, the new hexagon grid system is imposed on the image, as in (c). Each grid hexagon has a central hexagon H. From (c) to (d), the colour of a point in H, remains either colour 0 or 1. All other points have their colour advanced by 1. Thus from (c) to (d), orange hexagons are replaced by green hexagons with a central orange hexagon, and red hexagons are replaced with orange hexagons with a

central red hexagon. In (e), (f) and (g), $N = 3, 4$, and 11 respectively. At stage N, the regions of colour N approach a tiling of the plane by a tessellation of Koch snowflakes of two sizes [2, 14]. Figure 12 illustrates

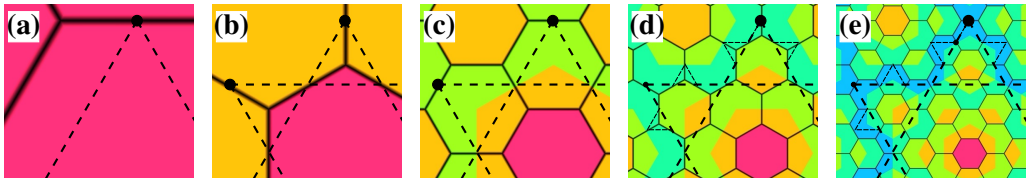

Figure 12: *Relationship between hexagons and the Koch snowflake.*

the relationship between the hexagons and the Koch snowflake. We see that if (after an odd number of operations) we join midpoints of adjacent edges in hexagons, provided they are entirely in a region with the maximal colour index, then we obtain iterates of the Koch snowflake. Thus we have a relationship between the terdragon curves and the Koch snowflake, illustrated for example in Figure 1.

Hinged Truchet Triangles

In this section a hinged triangle tessellations operation is applied as in Figure 13, or in the opposite direction of rotation. When maximally opened, as in Figure 13 (h), we divide the hexagon region into 6 triangles, as

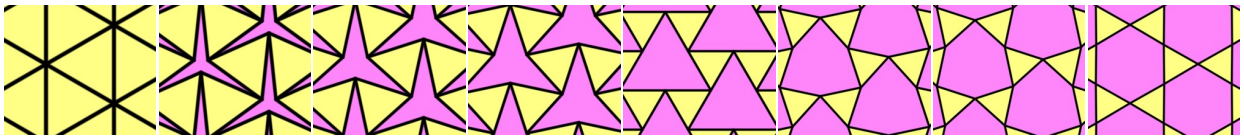

(a) $t = 0$ **(b)** $t = 0.1$ **(c)** $t = 0.2$ **(d)** $t = 0.3$ **(e)** $t = 0.5$ **(f)** $t = 0.7$ **(g)** $t = 0.8$ **(h)** $t = 1$

Figure 13: *Hinged triangle tiling, with triangles rotated through* $60t$ *degrees at stage* t*, for* $0 \le t \le 1$.

in Figure 14 (e). There are two operations, 0 and 1, depending on the rotation direction of the tiles. for both operations, adjacent tiles rotate in opposite directions. This results in replacing each original triangle with four smaller triangles, as in Figure 14 (d). The tiles are decorated with the Smith Truchet designs of Figure 2 right. There are two kinds of tiles, reflections of each other, which we call odd and even. Each tile has 3 possible orientations, as in Figure 2 right. Figure 14 shows example initial tilings, where the tile orientation is indicated by the tile background, blue, orange or white. The grey tiles in Figure 15 have an unspecified orientation, depending on the starting configuration. When the hinge operation (Figure 13) is applied to these

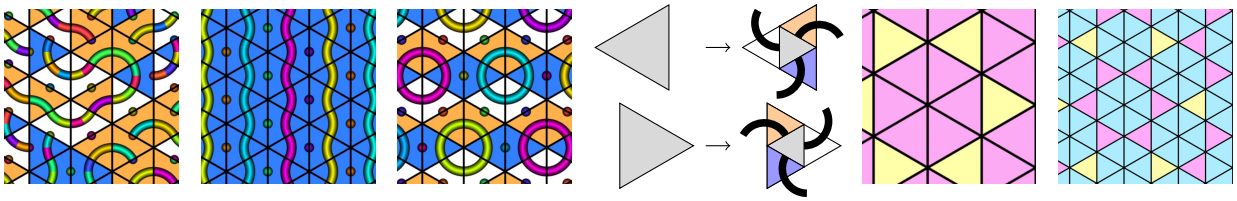

(a) **(b)** **(c)** **(d)** **(e)** **(f)**

Figure 14: *(a) – (c) Example initial tilings. (d) Replacement rule for operation* 0*. (e)* $t = 1$*. (f)* $t = 2$.

marked tiles, as in Figure 15, (a) to (b), there is a unique way to inert new tiles to preserve connected paths, as in (c) or (d). We can apply a sequence of operations to any initial arrangement. In Figure 16, (a) shows an initial tiling; (b) is the result of applying operation 0 once; (c) the result of six applications of operation 0. After each application of an operation, a single dot is transformed into a single curve, as in (b). In (d),

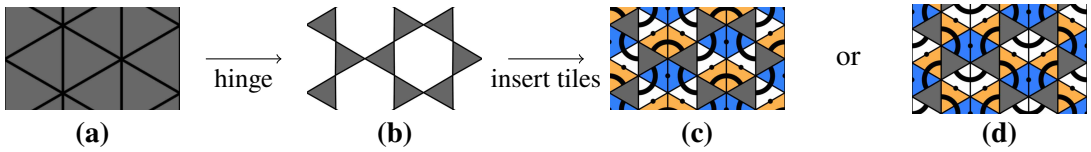

Figure 15: *Insertion rules, for operations* 0 *or* 1 *respectively.*

for clarity, these new paths are left out, which shows the result after 4.5 applications of operation 0, that is, apply operation 0 four times, and then apply a further half way opening of operation 0, to the extent as in Figure 13 (e), where $t = 0.5$, i.e., the triangles have been rotated through 30°. See also [10, Figures 28 and 34]. For operation sequence $000\ldots$, we see the appearance of the Sierpinski triangle. Changing the operation sequence will give a different fractal, e.g., (e) and (f) correspond to sequences of operations 10101

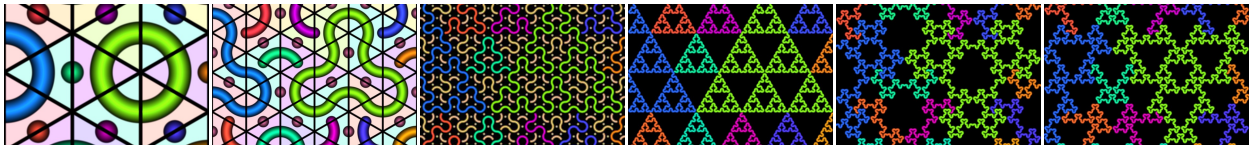

Figure 16: *Sierpinski variations obtained from the hinged triangle operation. For (a)–(d) the operation sequence is* 00000*. For (e) and (f) the sequences are* 10101 *and* 11000 *respectively.*

and 11000 respectively. We may consider members of this family, corresponding to arbitrary infinite binary sequences, to be variations on the Sierpinski fractal. Further examples are given in [10]. Other Sierpinski variations are discussed in [8]. We can apply the same background colouring algorithm as in Figure 11. The result is a Sierpinski triangle, as a colouring of Pascal's triangle, with a mod 2^N colouring scheme. Some examples are shown in Figure 17. An explanation of why the Sierpinski triangle is produced by the operation

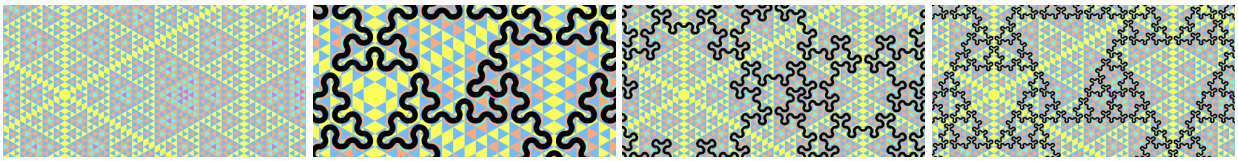

Figure 17: *Result of background colouring algorithm, with no curve, and curves corresponding to operation sequences* 1100, 10101, 110001*, and* $t = 5, 4, 5, 5.9$*, respectively.*

sequence $000\ldots$ is given in [10]. Other binary sequences will give other fractals. In [10] a further "hinged triangle tiling version 2" is discussed, which produces the boundary of the terdragon curve, as in Figure 18, the fudgeflake [3, p. 23], and an infinite family of fractals, one corresponding to each binary sequence.

Summary and Conclusions

We have recreated several well known fractals, giving new insight into them and relationships between them, and natural ways of incorporating certain different fractals in the same art works, as in Figure 1. We can also vary the iteration stage across the image, as in Figure 19 and examples in [10]. A summary of the L-system rules is as follows. The words are of the form $X - X - X \cdots$ for the hexagon case, and $XeXoX\ldots$ for the triangle cases, as explained in [10]. In each case, the L-system maps $R \to R$ and $L \to L$. The remaining rules are as in Table 1. In each case, there is an infinite family of related curves. Further explanations and examples of art work produced by these operations can be found in [10]. There are many other hinged tilings

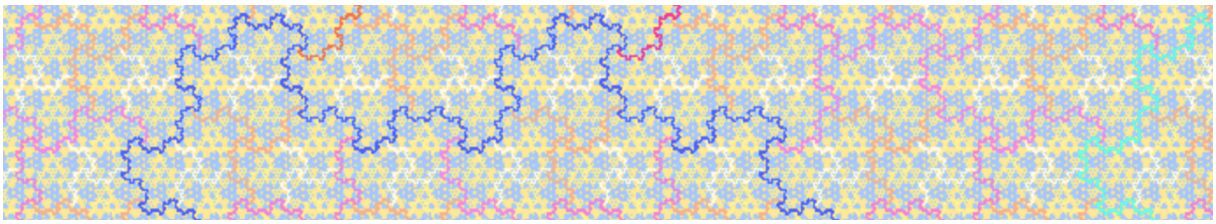

Figure 18: *The boundary of the terdragon produced from a hinged triangle tiling procedure.*

Table 1: *Summary of L-systems*

Tiling	Hexagon	Triangle 1	Triangle 2
operation 0	$- \to -L - R-$	$e \to oReRo$	$e \to oLe$
		$o \to eLoLe$	$o \to oRe$
operation 1	$- \to -R - L-$	$e \to oLeLo$	$e \to oRe$
		$o \to eRoRe$	$o \to oLe$
result, variants of:	terdragon	Sierpinski triangle	terdragon boundary

to apply variations of these methods to. For example, the method used here to produce the boundary of the terdragon can be modified to give the boundary of the Heighway dragon [12].

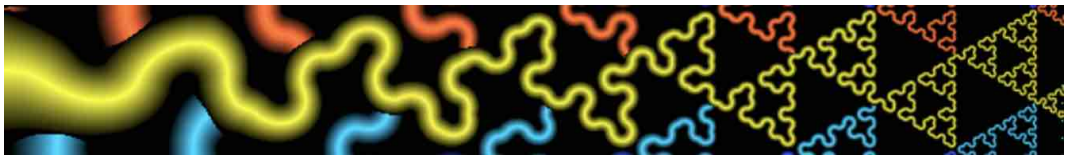

Figure 19: *Variable level iteration applied to hinged triangle Truchet tiling, operation* 0 *only.*

References

[1] J. Arndt and J. Handl, "Edge-covering plane-filling curves on grid colorings: a pedestrian approach". *arXiv:2312.00654,[math.CO] Dec. 2023. https://arxiv.org/abs/2312.00654.*

[2] A. Burns, "Fractal tilings". *Mathematical Gazette.* vol. 78 (482), pp. 193–6. 1994.

[3] G. Edgar. *Measure, Topology, and Fractal Geometry*. Undergraduate Texts in Mathematics. Springer, 2008.

[4] A. Flores. *Hinged Tilings*. https://www.public.asu.edu/~aaafp/tiling/hingedtilingtext.html

[5] G. Frederickson. *Hinged dissections: Swinging and twisting*. Cambridge University Press, 2002.

[6] S. Tabachnikov. "Dragon Curves Revisited". *Math. Intelligencer*, vol. 36, no. 1, 2014, pp. 13–17.

[7] T. Tarnai, P. Fowler, S. Guest and F. Kovacs. "Equiauxetic Hinged Archimedean Tilings." *Symmetry (Basel)*, vol, 14 (2), 2022.

[8] T. Taylor. "The Beauty of the Symmetric Sierpinski Relatives". *Bridges Conference Proceedings*, 2018, 163–170.

[9] H. Verrill. "Space Filling Truchet Variations". *Bridges Conference Proceedings*, 2023, pp. 465–468.

[10] H. Verrill. "Fractals from Hinged Hexagon and Triangle Tilings: Supplement". 2024.

[11] H. Verrill. *Hinged Truchet Tilings 2*. 2024. JavaScript program. https://www.mathamaze.co.uk/Truchet2/.

[12] H. Verrill. "L-systems for the Boundaries of Space Filling Folding Curves". 2024. *arXiv:2402.16106,[math.CO] Feb. 2024. https://arxiv.org/abs/2402.16106*

[13] Wikipedia. *Dragon Curve*. 2024. https://en.wikipedia.org/wiki/Dragon_curve.

[14] Wikipedia. *Koch snowflake*. 2024. https://en.wikipedia.org/wiki/Koch_snowflake

[15] Wikipedia. *L-system*. 2024. https://en.wikipedia.org/wiki/L-system.